Coupled-domain Nonlinear Macromodels and Pull-in Characteristics with Electro-Thermal Effect

Szu-Yuan Cheng, Che-Chia Yu and Yao-Joe Yang
Department of Mechanical Engineering
National Taiwan University, Taipei, Taiwan, ROC
giga@mems.me.ntu.edu.tw

Abstract

In this paper, we describe an efficient coupled-domain nonlinear macromodeling method for microsystems, and present the study of electro-thermal effects on the pull-in characteristic for a fixed-fixed beam by using this approach. The macromodeling method applies both the Karhunen-Loeve/Galerkin technique and the Arnoldi technique. The compact models generated by these two techniques are successfully integrated and tested. The application of the macromodels are demonstrated and discussed. Experimental verification for the simulated results is also provided.

1. Introduction

System-level simulations of MEMS devices are essential for dynamic performance prediction and optimization. One of the key requirements for such simulations is the development of efficient and accurate macromodels that are compatible with system-level solvers. Since most MEMS devices are nonlinear coupled-domain systems, various techniques for extracting macromodels from different energy domains have been proposed. For linear or weakly nonlinear systems, the macromodels can be easily obtained by reducing the finite-element (FEM) or finite-difference (FDM) formulations using the Arnoldi or the quadratic techniques [1][2]. These approaches are very efficient and accurate for linear systems. However, their errors are extremely large for nonlinear systems. Rewienski [3][4] proposed an algorithm which piecewise-linearly links the linear compact models generated by the Arnoldi method at different operating points. This algorithm smartly evaluates the weighting of each linear macromodel based on the error between the training trajectory and the operating trajectory. Under the condition that the training trajectory is close to the actual operating trajectory, this algorithm have been proved to be efficient and accurate for highly nonlinear system. The reduced order models generated by the Karhunen-Loeve/Galerkin approach [5][6][7], on the other hand, is based on the basis functions extracted from an ensemble of snapshots of physical fields (e.g., pressure distribution or temperature distribution), and are very useful for nonlinear systems with arbitrary operation conditions. However, this approach requires extremely expensive coupled-domain FEM/FDM runs to provide enough data snapshots. Furthermore, The effort on implementing and simulating the FEM/FDM runs increase exponentially if any new physical domains are introduced.

In this work, we demonstrate a macromodeling procedure which combines the compact models generated by both the Karhunen-Loeve/Galerkin and the Arnoldi methods. For the nonlinear domains, such as structural dynamics and fluidic damping effect, the Karhunen-Loeve/Galerkin method is used. For the linear domain, such as the thermoelectric effect, the Arnoldi algorithm is applied to generate the reduced order models. A simulated MEMS example, which includes structural mechanics, squeeze-film damping effect, electrostatics and thermo-electric domains, will be demonstrated. The pull-in characteristic of the device is also studied and discussed.

2. Karhunen-Loeve Decomposition

The Karhunen-Loeve Decomposition technique was original developed for creating a set of basis functions from an ensemble of snapshots in order to represent a stochastic field with a minimum degree of freedom. In this work, this technique will be used to extract the basis functions of physical fields for coupled-domain MEMS systems. The brief description of the Karhunen-Loeve decomposition is as follows:

Given N arbitrary snapshots of shape functions v_n, where $n = 1,2...N$. The goal is to extract a few basis functions that capture characteristics of the v_n best. This process is equivalent to maximize:

$$\lambda = \frac{\left\langle (\varphi, v_n)^2 \right\rangle}{(\varphi,\varphi)} \tag{1}$$

where $(f,g) = \int_\Omega f(x)g(x)d\Omega$ is the inner product of the two functions f and g, $\langle v_n \rangle \equiv \frac{1}{N}\sum_{n=1}^{N} v_n(x)$ is the mean of snapshot ensemble.

The numerator of Equation 1 can be expanded as:

$$\begin{aligned}\left\langle (\varphi, v_n)^2 \right\rangle &= \left\langle \int_\Omega \varphi(x)v_n(x)dx \int_\Omega \varphi(x')v_n(x')dx' \right\rangle \\ &= \int_\Omega \left\{ \int_\Omega \langle v_n(x)v_n(x') \rangle \varphi(x)dx \right\} \varphi(x')dx'\end{aligned} \tag{2}$$

After rearrange Equation 1, the objective of maximize λ can be transform into an eigenvalue problem:

$$C_{nk}\alpha_k = \lambda\alpha_n \tag{3}$$

where $\varphi(x)$ is defined using the Schmidt-Hilbert technique:

$$\varphi(x) = \sum_k \alpha_k v_k(x) \tag{4}$$

and

0-7803-7731-1/03/$17.00 ©2003 IEEE

$$C_{nk} \equiv \frac{1}{N}\int_{\Omega} v_n^T(x')v_k(x')dx' \qquad (5)$$

Since C_{nk} is symmetric and positive definite, the eigenvectors of the Equation 3 can be substituted into Equation 4 to yield eigenfunctions φ_k. The eigenfunction corresponding to the largest eigenvalue is the most representative shape of fields extracted from the ensemble of the snapshots v_n, the eigenfunction corresponding to the second largest eigenvalue is the second most representative shape of fields, and so on [8]. In practice, the snapshots can be obtained from typical transient FEM/FDM simulations. Since only a few eigenfunctions (basis functions) are necessary to represent the dynamic behaviors accurately, they can be incorporated with the Galerkin method for reduced-order modeling.

3. Macromodeling using Galerkin Method

In the section, we use the eigenfunctions extracted by the Karhunen-Loeve Decomposition technique as the basis functions for the Galerkin method. The example studied is a fixed-fixed beam fabricated by the MUMPs® process, as shown in Figure 1. The electrostatic force distribution caused by the voltage difference (V1) between the beam and the bottom electrode actuates (pulls down) the beam. If the voltage exceeds a critical value, the pull-in voltage, the beam collapses onto the bottom electrode (pull-in). This mechanism is widely used in the switch-type devices. If another voltage source is connected between the two ends of the beam (V2), an electric current flowing through the beam results in Joule heating. The temperature increase caused by the heating expands the beam structure so that the pull-in characteristics, such as pull-in voltage and pull-in dynamics, will be changed.

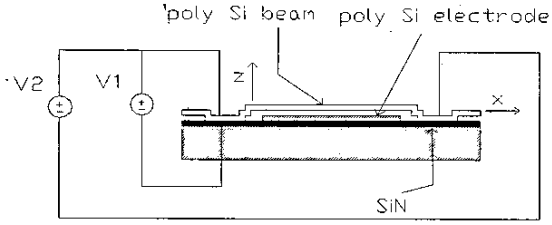

Figure 1. *The schematic of the device analyzed in this work.*

The fixed-fixed-beam system can be modeled by coupling a 1-D beam equation for structural dynamics, a 2-D Reynold's equation for squeeze-film damping, and a 3-D energy equation for heat transfer effect. The electrostatic force is included into a beam equation as a distributed load. The governing equations are shown below:

$$EI\frac{\partial^4 z}{\partial x^4} - (S - (\alpha_0 \Delta T - \varepsilon)AE)\frac{\partial^2 z}{\partial x^2} = F_{elec} + F_{air} - \rho\frac{\partial^2 z}{\partial t^2} \qquad (6)$$

$$\frac{\partial^2 T}{\partial x^2} + \frac{\partial^2 T}{\partial y^2} + \frac{\partial^2 T}{\partial z^2} + \frac{\dot{q}}{k} = \frac{1}{\alpha}\frac{\partial T}{\partial t} \qquad (7)$$

$$\nabla \cdot ((1 + 6Kn)z^3 p\nabla p) = 12\eta\frac{\partial (pz)}{\partial t} \qquad (8)$$

$$F_{elec} = \frac{-\varepsilon_0 \omega V^2}{2z^2}$$

where α_0 is the coefficient of thermal expansion, ε is the axial strain of the beam due to large deflection, $F_{air}(= \int_0^w (p - p_0)dy)$ is the resistant force caused by the squeeze-film damping, $z(x,t)$ is the displacement of the beam, $T(x,y,z,t)$ is temperature distribution of the beam, α is thermal diffusivity, $p(x,y,,t)$ is the pressure distribution inside the gap, p_0 is the ambient pressure, $Kn(= \lambda / z)$ is the Knudsen's number, $\lambda(= 0.064\mu m)$ is the mean free path of air, $E(= 149Gpa)$ is the Young's modulus, $I(= wh^3/12)$ is the moment of inertia of the beam cross-section, $w(= 40\mu m)$ is the width, $\rho / hw(= 2330kg/m^3)$ is the density of the beam (polysilicon), $\eta(= 1.82 \times 10^{-5})$ is the air viscosity, $l(= 610\mu m)$ is the beam length, and $h(= 2.2\mu m)$ is the beam thickness, and the residual stress of the beam is $S / hw(= -3.7Mpa)$. The initial gap between the beam and the bottom electrode is $z_0(= 2.3\mu m)$. The beam is fixed on both ends, while the air pressure on the both sides of the beam is fixed at ambient pressure.

The governing equations listed above include a linear partial differential equation (the energy equation) and two nonlinear partial differential equations (the beam equation and the Reynold's equation). For the linear equation, we use the Arnoldi technique [1] to generate compact models. Its theory and procedure can be found in [9][10][11][12]. For the nonlinear equations, we apply Karhunen-Loeve decomposition to extract basis functions, and use the Galerkin method to formulate reduced-order models.

The beam is discretized using finite difference formulations for the energy equation, which yields a set of ordinary differential equations:

$$\dot{x} = Ax + Bu$$

$$y = Cx$$

where x is the temperature at each node, u and y are the input and output respectively; A, B and C are matrices of the system. In this case, the C matrix is carefully formed that the output y will be the 1-D temperature distribution along x direction. Typically, the rank of the A matrix is close to the total number of the temperature nodes. The Arnoldi method is applied to reduce the system matrices A, B, C into much lower order (rank) matrices A_q, B_q, C_q.

For the beam equation and the Reynold's equation, we describe the displacement and the pressure distribution as the superposition of the basis functions (z_i or p_i) obtained by the Karhunen-Loeve Decomposition technique:

$$\hat{z}(x,t) = z_0 + \sum_{i=1}^{M} \beta_i(t) z_i(x) \qquad (9)$$

$$\hat{p}(x,y,t) = p_0 + \sum_{i=1}^{N} \alpha_i(t) p_i(x,y) \qquad (10)$$

Assume either of the partial differential equations is written as the following form.

$$L(u) = f \qquad (11)$$

where L is a differential operator, and u is the solution of field of the partial differential equation. The Galerkin condition requires that

$$(a_i, L(\hat{u}) - f) = \int a_i^T (L(\hat{u}) - f) dx = 0 \qquad (12)$$

$$i \in \{1,2,3,...,N\}$$

where a_i is either z_i or p_i in Equation 9 and 10.

Finally, Equation 12 yields two sets of ordinary differential equations which are reduced from the two original partial differential equations:

$$M\ddot{\beta} + K\beta + f = 0 \qquad (13)$$

$$P\dot{\alpha} + Q\alpha + r = 0 \qquad (14)$$

where $M_{ij} = \int_C \rho b_i b_j dx$

$$K_{ij} = \int_C \left(EI \frac{\partial^2 b_i}{\partial x^2} \frac{\partial^2 b_j}{\partial x^2} + (S - (\alpha_0 \Delta T - \varepsilon)) \frac{\partial b_i}{\partial x} \frac{\partial b_j}{\partial x} \right) dx$$

$$f_i = -\int_C b_i (F_{elec} + F_{air}) dx$$

$$P_{ij} = \int_S 12\eta a_i a_j \hat{z} dx dy$$

$$Q_{ij} = \int_S \left((1 + 6Kn)\hat{z}^3 \hat{p} \left(\frac{\partial a_i}{\partial x} \frac{\partial a_j}{\partial x} + \frac{\partial a_i}{\partial y} \frac{\partial a_j}{\partial y} \right) + 12\eta a_i a_j \frac{\partial \hat{z}}{\partial x} \right) dx dy$$

$$r_i = \int_S 12\eta p_0 a_i \frac{\partial \hat{z}}{\partial x} dx dy$$

Since the order of Equations 13 and 14 are mthus the computational cost is much lower than the typical FEM/FDM solvers that simulate the two governing equations.

4. Results

The full model is meshed into FDM model with 3321 nodes (41 for the beam equation, 820 for the Reynolds equation, and 2460 for the energy equation). This fully-meshed FDM model is ready for computing the coupled effects of the system. However, if using the Karhunen-Loeve technique solely, the computational cost will be too expensive to efficiently extract the global basis functions. Instead, we apply the Karhunen-Loeve technique only for the structural dynamics and squeeze-film damping effects, while use the Arnoldi technique to reduce the heat equation into macromodels.

Figure 2 shows a good agreement between the results by the FDM solver and the macromodel for the beam under steady volume heat generation. Figure 3 indicates that the errors are below 1% for the macromodel used in Figure 2. Table 1 shows the comparison of average error, computation time and speed-up factor between the full-FDM, the FDM with a heat-transfer macromodel, and the full macromodels. This figure not only shows that the macromodels accelerate the simulations, but also indicates that the cost of using Karhunen-Loeve technique to generate macromodels increases significantly if the energy equation is included. Under a constant volume heat generation rate, the temperature distribution along the beam calculated by the macromodel is shown in Figure 4. Figure 5 shows the effect of heat generation rate on the pull-in time under different applied voltage. Since the temperature increase of the beam induces thermal strain, the pull-in time is reduced. Also, the pull-in voltage can be effectively reduced if higher volume heat generation rate is applied. Figure 6 shows the comparison of the measured (using interferometer) and simulated results for the beam under an applied voltage of 4 volts.

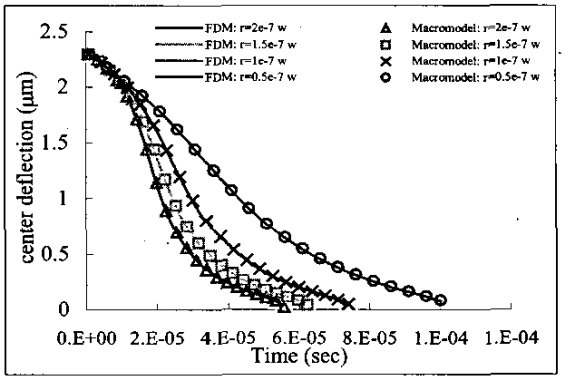

Figure 2. *The comparison of FDM and the macromodel for M=2, N=4 and q=5, where M and N are the numbers of the basis functions for the beam equation and the Reynold's equation, respectively; q is the order of the system reduced from the thermal equation. Pull-in voltage is 8 volts and r is the heat generation rate.*

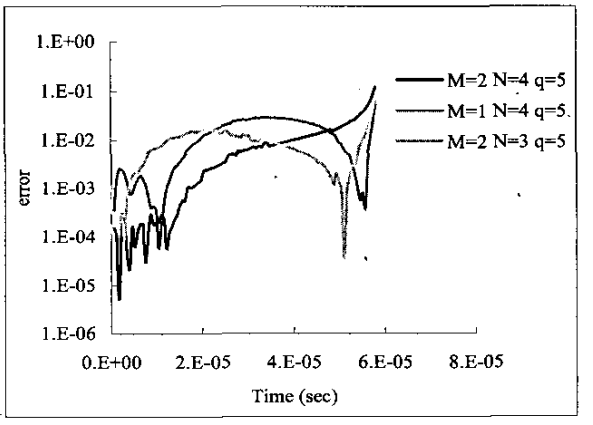

Figure 3. *Comparison of errors with different numbers of basis functions.*

Models	Average error	Comp. time (s)	Speed-up factor
Fully-meshed FDM method	N/A	8535	1.0
FDM (beam+Reynold's+electrostatic) with Macromodel (thermal, q=5)	<<0.1%	148	57.7
Macromodels (M=2, N=4, q=5)	0.9%	17	502.1
Macromodels (M=2, N=3, q=5)	0.9%	9	948.3
Macromodels (M=2, N=2, q=5)	5.5%	4	2133.8

Table 1. *The comparison of average error, computation time and speed-up factor between the full-FDM, the FDM with a heat-transfer macromodel, and the macromodels.*

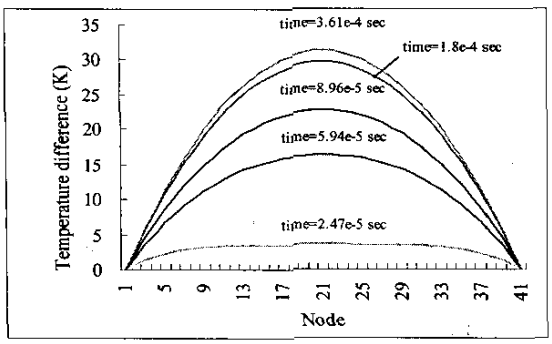

Figure 4. *The distribution of temperature along the length of the beam. The heat generation rate is 1e-7 w at every node.*

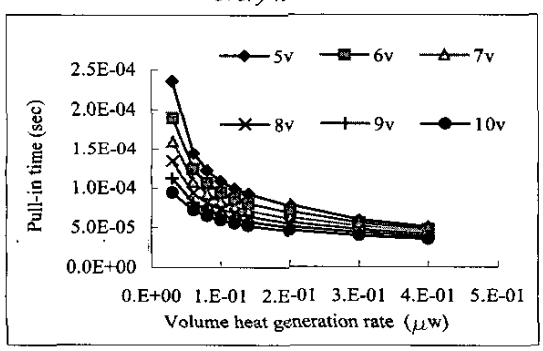

Figure 5. *Volume heat generation rate versus pull-in time under different pull-in voltage.*

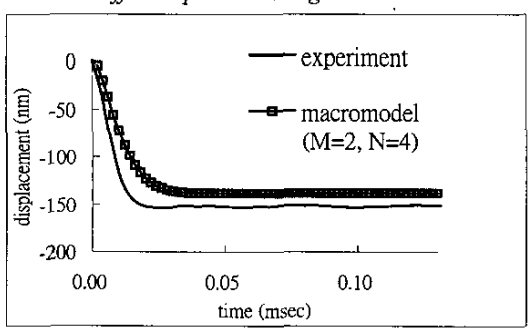

Figure 6. *Comparison of measured and simulated results for the beam under an applied voltage of 4 volts.*

5. Conclusion

This paper presented an approach of simulating the coupled-domain microsystems using various reduced order modeling techniques. For nonlinear domains, the Karhunen-Loeve decomposition technique is used to extract basis function, and the Galerkin method is used to formulate reduced-order model. For the linear domain, the Arnoldi-based technique is used to generate compact models. The theories of the techniques are described briefly. A fixed-fixed-beam microsystem, which includes structural dynamics, squeeze-film damping, heat transfer and electrostatics domains, is modeled using this approach. The simulated results indicate that the pull-in dynamic characteristic can be control by the Joule heating effect. Measured transient displacement of the beam also verifies the simulated results.

Acknowledgement

This work is partially supported by the NSC (National Science Council, Taiwan, ROC) through the Grant contact No: NSC-90-2218-E-002-031.

References

[1] F. Wang and J. White, "Automatic Model Order Reduction of a Microdevice using the Arnoldi Approach," *ASME IMECE 98*, DSC-Vol. 66, pp527-530.

[2] Y. Chen and J. White, "A Quadratic Method for Nonlinear Model Order Reduction," *Modeling and Simulation of Microsystems*, pp. 477-480, 2000.

[3] M. Rewienski, J. White, "A Trajectory Piecewise-Linear Approach to Model Order Reduction and Fast Simulation of Nonlinear Circuit and Micromachined Devices," *Computer-Aided Design*, pp.252-257, 2001.

[4] M. Rewienski, J. White, "Improving Trajectory Piecewise-Linear Approach to Nonlinear Model Order Reduction for Micromachined Devices Using an Aggregated Projection Basis," *Modeling and Simulation of Microsystems*, 2002.

[5] E. Hung and S. Senturia, "Generating Efficient Dynamical Models for Microelectromechanical Systems from a Few Finite-Element Simulation Runs," *Journal of Microelectromechanical Systems*, Vol. 8, No. 3, September 1999.

[6] J. Chen and S. Kang, "An Algorithm for Automatic Model-Order Reduction of Nonlinear MEMS Devices," *Circuits and Systems*, May 28-31, 2000.

[7] Arieh Iserles, A First Course in the Numerical Analysis of Differential Equations, Cambridge University Press, 1996.

[8] Gene H. Golub and Charles F. Van Loan, Matrix Computations, The John Hopkins University Press 1996.

[9] Microsystem Design, Stephen D. Senturia, Kluwer Academic Publishers, 2001.

[10] Y.-J. Yang, et. al., "Modeling Gas Damping and Spring Phenomena In MEMS With Frequency Dependent Macro-Models," *IEEE MEMS 2001*.

[11] Stephen P. Timoshenko and S. Woinowsky-Krieger, Theory of Plates and Shells, McGraw-Hill, 1959.

[12] Singiresu S. Rao, Mechanical Vibrations, Addison-Wesley Publishing Company, 1990.